# HYDROPHOBIC SURFACE OF Zn-Al-WO<sub>3</sub> HOT DIPPED GALVANISED COATING MODIFIED WITH DIFFERENT MOLARITY OF STEARIC ACID

Mohd Nazri Idris\*, Devah Kalai Selvam, Nik Akmar Rejab, Zuhailawati Hussain and Anasyida Abu Seman

School of Materials and Mineral Resources Engineering, Engineering Campus, Universiti Sains Malaysia, 14300 Nibong Tebal, Pulau Pinang, Malaysia

\*srmnazri@usm.my

**Abstract.** Hot dip galvanizing is the oldest and most cost-effective corrosion resistance method for steel, acting as both a physical barrier and a sacrificial effect. Galvanised steel, on the other hand, corrodes when exposed to harsh environments over time. Thus, increasing the hydrophobicity of galvanised steel can reduce corrosion rates and increase service life. The purpose of this study is to investigate the effect of stearic acid on the formation of a hydrophobic structure of Zn-Al-WO<sub>3</sub> on mild steel. Hot dip galvanizing was used to coat the Zn-Al-WO<sub>3</sub> on mild steel. The coated sample was surface treated with stearic acid in varied molarities ranging from 0.002 to 0.05 M. The surface treated coating was analyzed using scanning electron microscopy (SEM), field emission scanning electron microscopy (FESEM) equipped with energy dispersive X-ray (EDX), water contact angle (WCA), and atomic force microscopy (AFM). The corrosion resistance after surface treatment was assessed using the potentiodynamic polarization method in a 3.5% NaCl solution. The results demonstrate that the 0.008 M stearic acid had a greater WCA at 122.29° with a surface energy of 10.42 mJ.m<sup>-2</sup>. This 0.008 M stearic acid also provided the best surface roughness and corrosion rate, with minimum values of 21.30 nm and 0.707 mmyr<sup>-1</sup>, respectively. This study found that 0.008 M is the ideal concentration of stearic acid for modifying the hydrophobic surface and can be employed for Zn-Al-WO<sub>3</sub> galvanised coating.

**Keywords:** Hydrophobic, stearic acid, molarity, hot dip galvanizing

## **Article Info**

Received 17<sup>th</sup> September 2023 Accepted 5<sup>th</sup> December 2023 Published 20<sup>th</sup> December 2023

Copyright Malaysian Journal of Microscopy (2023). All rights reserved.

ISSN: 1823-7010, eISSN: 2600-7444

## Introduction

Steel is extensively employed in engineering applications due to its cost-effectiveness, widespread availability, manufacturing flexibility, and superior mechanical strength. However, its susceptibility to corrosion significantly impacts its performance and service life in applications such as automotive, construction, marine, and oil and gas industries. Corrosion in steel occurs through chemical or electrochemical reactions between the steel surface and oxygen. Various strategies are employed to enhance steel corrosion resistance, including cathodic protection, anodic protection, the use of inhibitors, and the application of metallic coatings [1]. Zinc coatings are commonly utilized for steel protection, with methods such as hot-dip galvanizing, electroplating, spraying, mechanical plating, and painting. Among these, hot dip galvanizing stands out as the most efficient method, offering favourable mechanical properties, ductility, low density, corrosion resistance, cost-effectiveness, and recyclability [2]. However, galvanized steel is prone to corrosion when exposed to high humidity and corrosive atmospheres, leading to the formation of a corrosive electrolyte film on the surface that accelerates corrosion, resulting in white rust [3].

In marine industries, aggressive ions can rapidly corrode galvanized steel. To improve the performance of zinc coatings, various metal oxides or mixed oxides are added to the galvanic bath, enhancing the alloying characteristics of Zn-Fe alloy phases and creating a hydrophobic structure. Several elements, such as Mg, Al, Ni, Ti, Sn, and Pb, can be added to the zinc bath. The addition of Al inhibits the growth of Fe-Zn phases. The addition of additives, including metal oxides and mixed oxides, plays a crucial role in improving the alloying characteristics of Zn-Fe alloy phases. This leads to the formation of enhanced inner alloy structures, making the process more economical by reducing zinc consumption [4]. The incorporation of metal oxides, such as TiO2, Al2O3, ZrO2, ZnO, and CeO2, in hot-dip zinc coatings improved galvanic performance and corrosion resistance [5]. Research by Deepa et al. [6] suggests that even a small amount of these metal oxides can have a positive impact. Arumina et al. [7] discovered that adding 0.2 wt.% of tungsten oxide (WO<sub>3</sub>) nanoparticles to hot-dip zinc aluminium (Zn-0.1wt.% Al) resulted in a hydrophobic surface with a contact angle of 112.3° and a low corrosion rate of 6.54 ×10<sup>-6</sup> mmpy<sup>-1</sup>. WO<sub>3</sub>, being an n-type semiconductor material with a band gap of ~2.6–2.8 eV, offers improved coating characteristics. Additionally, WO<sub>3</sub> has been found to combat biocorrosion and enhance antibacterial activity in marine environments [8]. Moreover, in metal composites, WO<sub>3</sub> provides chemical stability in harsh environments.

Hydrophobic coatings are gaining popularity as a technique to improve the corrosion resistance of metallic substrates while also providing functionality such as self-cleaning, anticing, oil water separation, anti-fouling, and so on [9]. These coatings are based on the natural surface of lotus leaves, which have nano-structured surfaces coated with low-surface-energy compounds that operate as an interface between the coating and the liquid. The interface is created by maintaining air within the surface nano-scale topography, which reduces the contact area of water droplets and results in a non-wetting and low-adherence surface [10]. Hydrophobic coatings on galvanised steel can be created in one-step or two-steps method. The first stage in the two-step procedure is roughening the metal surface to produce micro or nano size structures either physically or chemically, followed by lowering surface energy by modification methods [11]. In a single procedure, hydrophobic coatings can be created via electrodeposition, solution immersion, laser irradiation, hydrothermal treatment, and other ways. This technology inspired researchers and companies by allowing for optimized scale-up production, eliminating the requirement to reduce material surface energy, and making the

process more simple, efficient, environmentally friendly, and time efficient. This approach also promises a high level of superhydrophobicity, with a minimum contact angle of 150° and a maximum sliding angle of 10° [9]. Naing et al. [12] shown that a superhydrophobic layer enhances the corrosion resistance of hot-dip galvanised steel substantially.

Liang et al. [9] effectively developed superhydrophobic property by surface treatment of 0.05 M stearic acid in ethanol solution followed by addition of 1 wt.% SiO2 on superhydrophobic coating, achieving contact angle of 160.12°. Stearic acid is a common surface modification reagent used to induce superhydrophobicity. It is also known as saturated fatty acid with the molecular formula C<sub>18</sub>H<sub>36</sub>O<sub>2</sub>. Stearic acid has a low surface energy and the capacity to generate feather-like zinc stearate structures to improve hydrophobic surfaces. Other research by Zhang et al. [13] shown that superhydrophobic films produced on mild steel for corrosion protection by mixing electrodeposited SiO<sub>2</sub> and durable polydimethylsiloxane (PDMS) display up to 99.99% corrosion prevention effectiveness in 3.5 wt% NaCl solution. Hu et al. [14] developed a superhydrophobic coating in two steps, beginning with a modified Zn coating with micro/nanostructures by electrodeposition and concluding with 0.02 M stearic acid in ethanol, yielding a water contact angle of 158.7° and a sliding angle of 6.4°. Furthermore, Hu et al. [15] investigated the effects of 0.008 M stearic acid for 5 hours on a coating of Fe<sub>2</sub>O<sub>3</sub>/Fe<sub>3</sub>O<sub>4</sub> composite film on N80, revealing a superhydrophobic property with a water contact angle of 159.6° and a sliding angle of 2.2°. Li et al. [16] use 0.05 M stearic acid in ethanol after etching with cupric hydrate solution to generate a superhydrophobic surface on galvanised steel with a water contact angle of 164.3°. Gurav et al. [17] investigated ZnO coated on glass substrates using the sol-gel dip coating method and surface treatment by varying the stearic acid molarity from 1 mM to 10 mM. The surface of the ZnO nanorods modified with 8 mM stearic acid showed a water contact angle of 152° and a sliding angle of 9°. The stearic acid surface modification can create low surface energy. However, the effect of acid stearic acid has been thoroughly explained. Thus, the aim of this research is to investigate the effect of different molarities of stearic acid on formation hydrophobic Zn-Al-WO<sub>3</sub> galvanised coatings. SEM, FESEM, EDX, WCA, and AFM were used to examine the surface property. The potentiodynamic polarisation technique was used to assess corrosion of a hydrophobic Zn-Al-WO<sub>3</sub> coating in a 3.5% NaCl solution.

# **Materials and Methods**

Mild steel plate with chemical composition (in wt.%) 0.08 P, 0.05 Si, 0.01 Ni, 0.27 Mn, 0.12 C, 0.05 S and the remainder iron was cut into a 10 x 50 x 0.5 mm shape with a cutting machine and drilled with a 3 mm hole on top of the sample. All samples were ground with silicon carbide grits ranging from 240 to 2000. To remove oil and grease, the mild steel samples were degreased for 10 minutes with 5 wt.% sodium hydroxides, NaOH, and rinsed with distilled water. The sample was then pickled in 8% hydrochloric acid, HCl for 15 minutes at room temperature to ensure the oxide layers were completely removed. The mild steel sample was then fluxed in a 30% ammonium chloride, NH4Cl solution for 15 minutes to prevent further oxidation on the sample surface and improve adhesion for hot dip galvanising. Following cleaning, the sample is thoroughly dried in hot air. A zinc ingot containing 98.8% Zn and 1 wt.% Al was melted at 550 °C to make the galvanic bath. Then, 0.2 wt% tungsten oxide, WO<sub>3</sub> powder was added to the Zn-Al molten mixture and stirred until all the WO<sub>3</sub> powder was completely dissolved. The mild steel was then submerged in the galvanic bath for 2 minutes using a pulley system before being gradually removed and the surplus molten Zn was removed

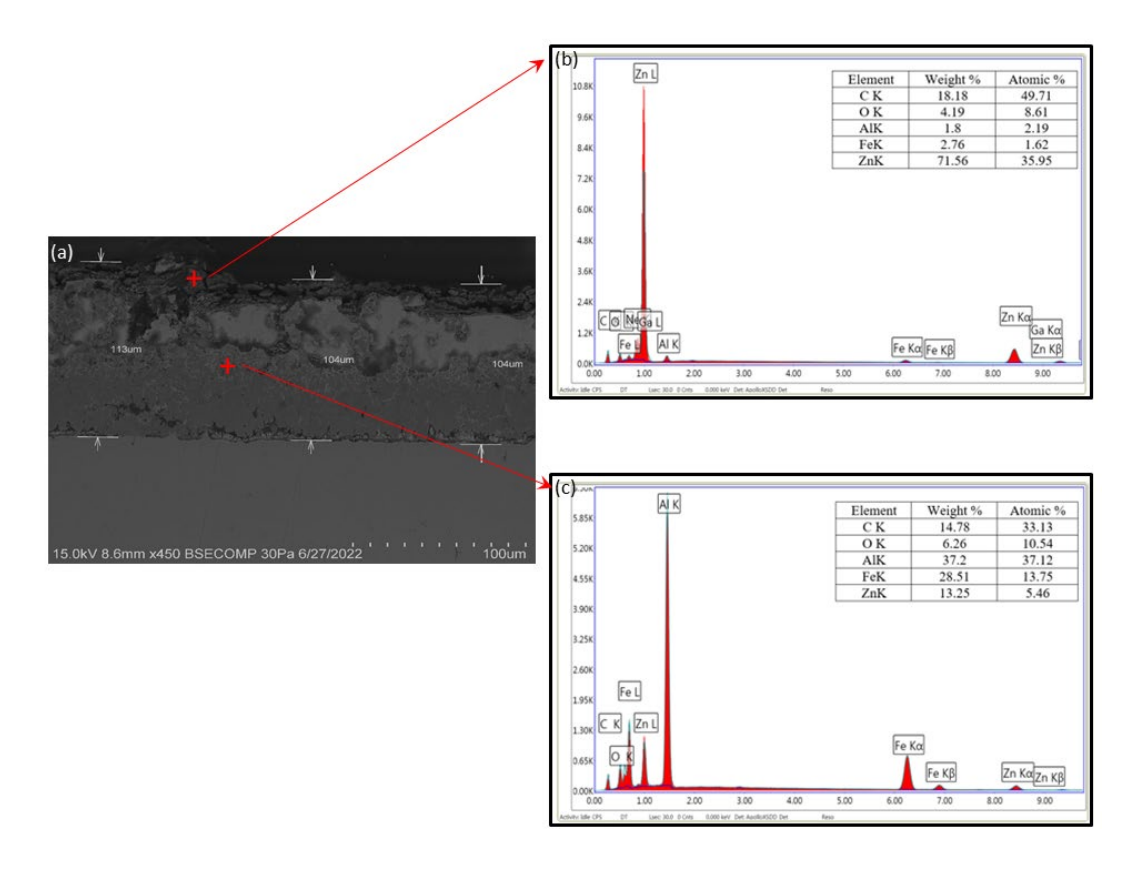
using hot air blowing. After galvanizing, the samples were allowed to cool to room temperature.

The galvanised sample was cut into 10 x 10 mm squares and ultrasonically cleaned for 15 minutes. The galvanised samples were tied with string and immersed in a solution containing various molarities of stearic acid (0.002 M, 0.005 M, 0.008 M, 0.01 M, 0.02 M, and 0.05 M) with 0.1 wt.% SiO<sub>2</sub> in ethanol for 2 hours. Following immersion, the samples are dried with hot air and stored in a dark, clean box. The morphology of treated samples was examined using a tabletop SEM model Hitachi TM 3000 and FESEM model LEO SUPRA 55VP attached with EDX. A goniometer was used to assess the hydrophobicity and surface energy of the coated sample, and AFM was used to analyse the surface roughness. The corrosion resistance of the treated coated surface was determined using the potentiodynamic polarisation technique in a 3.5 wt% NaCl solution. A typical three-electrode setup was employed, with a saturated calomel electrode (SCE), a platinum rod, and a sample serving as the reference, counter, and working electrodes, respectively. This test was analysed using the potentiostat/galvanostat Model PGSTAT101 and the NOVA 10 software. Tafel polarisation was measured at a scan rate of 1 mVs<sup>-1</sup> throughout a potential range of -0.25 to 0.25 V versus open circuit potential. To guarantee the repeatability of the results, all samples were examined in triplicate.

## **Results and Discussion**

## Morphology Analysis

Figure 1(a) depicts the FESEM microstructure of galvanised steel having Zn-Al-WO<sub>3</sub>. The coating has an average thickness of 107 µm, which is less than the thickness of pure Zn coating. The incorporation of WO3 nanoparticles interacts with zinc during hot-dip galvanization to generate W-Zn, which has higher bond energies than Fe-Zn. This W-Zn arrangement creates more compact adherent layers and reduces coating thickness [5]. Furthermore, the addition of 1 wt% Al results in the formation of the Fe<sub>2</sub>Al<sub>5</sub>Zn<sub>x</sub> (η) phase, which inhibits the formation of Fe-Zn intermetallic compounds. Deepa et al. [6] discovered that if Al content is greater than 0.14 wt%, Fe<sub>2</sub>Al<sub>5</sub> is thermodynamically stable and fully inhibits the n phase of Fe-Zn. According to the EDX results at the inhibitory layer (Figure 1(c)), the weight of aluminium is 37.2%, followed by iron (28.51%), and a trace of zinc (13.25%). This indicates the strong bonding of the Al-Fe interaction at this point. Although aluminium has a stronger affinity than zinc for the formation of Al-Fe bonds, it cannot completely impede the formation of intermetallic Zn-Fe phases but reduced the growth of the layer. A trace of zinc diffuses through the inhibitory layer Fe<sub>2</sub>Al<sub>5</sub> and creates a trace of the Fe-Zn intermetallic phase. According to the EDX results in Figure 1(b), the bulk of zinc (71.56%) is present in the outer layer, with very little iron (2.76%) and aluminium (1.8%) present. The presence of carbon and oxygen is due to contamination from the graphite crusibel used in this procedure. In this hot dip Zn-Al-WO<sub>3</sub> galvanised, the eta phase has entirely covered the outer layer of coating.



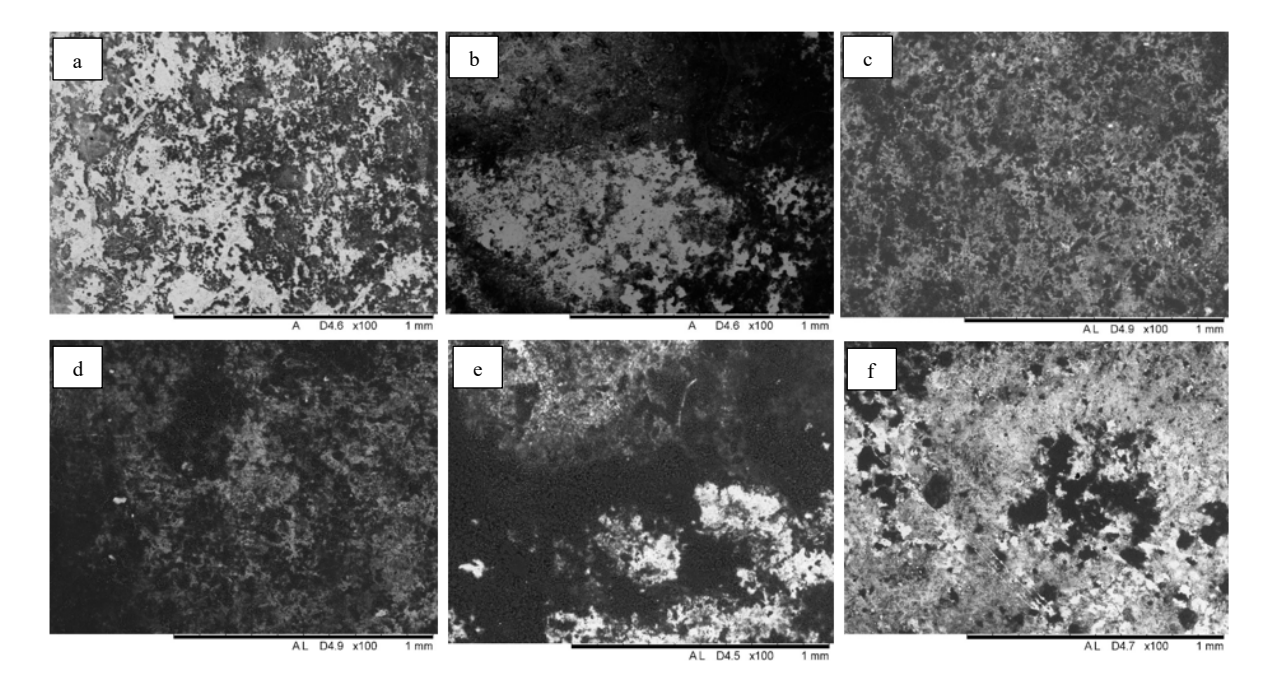
**Figure 1:** (a) Cross-sectional microstructure of galvanised steel and EDX results for (b) inhibition layer and (c) outer zinc layer

Figure 2 depicts the SEM morphology of surface-modified samples with varying stearic acid molarities. Stearic acid with a molarity of 0.008 M (Figure 2(c)) has a homogeneous distribution of zinc stearate covering the surface of the samples. Stearic acid has a low surface energy because it is made up of a long alkyl chain with a carboxy head group. This carboxy molecule is very reactive and capable of reacting with zinc ions from the surface coating, resulting in the formation of a feather-like structure zinc stearate [6]. The addition of additional SiO<sub>2</sub> nanoparticles changes the structure of zinc stearate into a feather-like lamellar structure [6]. The molarities of 0.002 M and 0.005 M have inadequate concentrations of stearate ions to react with zinc, resulting in less zinc stearate production and inability to completely cover the surface of samples. In ethanol solution, excess stearic acid began aggregating into irregular shapes at molarities greater than 0.01 M. As can be seen in Figure 2(e) and (f), the rate of agglomeration increases as the concentration of stearic acid in ethanol rises.

# Contact Angle Measurement

The goniometer was used to measure the contact angle and surface energy of the coated samples. As indicated in Table 1, sample modified with stearic acid at 0.008 M exhibited a maximum contact angle of 122.29° and a surface energy of 10.42 mJ.m<sup>-2</sup>. The contact angle was lower (93.76°) at a low molarity of 0.002 M and steadily grew as molarity increase to 0.008 M. However, when the molarity of stearic acid increases beyond 0.01 M, the water contact angle gradually drops to the lowest hydrophobic level (90.92°), and their surface energy values are less significant compared to 10.42 nm at 0.008 M stearic acid utilised. Stearic acid reacts with the zinc layer to generate zinc stearate, which has a low surface energy and a high-water repellency. At 0.008 M concentration, the modified zinc stearate surface trapped more air and

reduced the contact area between water and the Zn-Al-WO<sub>3</sub> galvanised coating. At this 0.008 M concentration, the developing zinc stearate feather-like lamellar homogeneously covers the droplet, generating nanoscale roughness that traps air and produces a solid-air-liquid interface, increasing the water contact angle, as anticipated by the Cassie-Baxter model [9]. However, when the concentration of stearic acid exceeds 0.01 M, the rate of agglomeration rises, resulting in poor zinc stearate dispersion [15]. As a result, the hydrophobicity of zinc stearate drops to 33.32% at 0.05 M stearic acid concentration.



**Figure 2:** Morphology of galvanised steel after surface treatment under various molarity of stearic acid (a) 0.002 M, (b) 0.005 M, (c) 0.008 M, (d) 0.01 M, (e) 0.002 M and (f) 0.005 M

Table 1: Contact angle for various molarity of stearic acid

Water contact angle Surface

Molarity	Water contact angle	Surface energy	
(M)	()	$(mJ.m^{-2})$	
0.002	$93.76 \pm 0.01$	$26.88 \pm 0.01$	
0.005	$102.93 \pm 0.35$	$21.27 \pm 0.21$	
0.008	$122.29 \pm 0.02$	$10.42 \pm 0.01$	
0.01	$110.19 \pm 0.98$	$16.98 \pm 0.56$	
0.02	$107.09 \pm 0.03$	$18.79 \pm 0.02$	
0.05	$90.98 \pm 0.02$	$28.61 \pm 0.01$	

## Surface Roughness

According to the topography in Figure 3, 0.008 M stearic acid has a more homogeneous structure than other molarities. Table 2 shows that the average surface roughness reported for 0.008 M was 21.30 nm. This demonstrates that samples that have been surface modified with 0.008 M stearic acid have consistent roughness throughout the coating's surface area. In other molarities, the surface is not equally distributed, with some areas having high roughness and others being smooth, affecting the average surface roughness value. Table 2 reveals that the surface roughness value of stearic acid surface modified samples is 45.88 nm at 0.05 M concentration. The high stearic acid concentration causes a substantial quantity of surplus

stearate crystal and SiO<sub>2</sub> nanoparticles to combine into irregular shapes, resulting in greater roughness in certain locations and an increase in the average surface roughness value. As a result, the surface roughness is not homogeneous over the coated sample's surface area. This study agreed well with the supplied morphology in Figure 2, where changes in morphology as stearic acid concentration increased influenced surface roughness measurement.

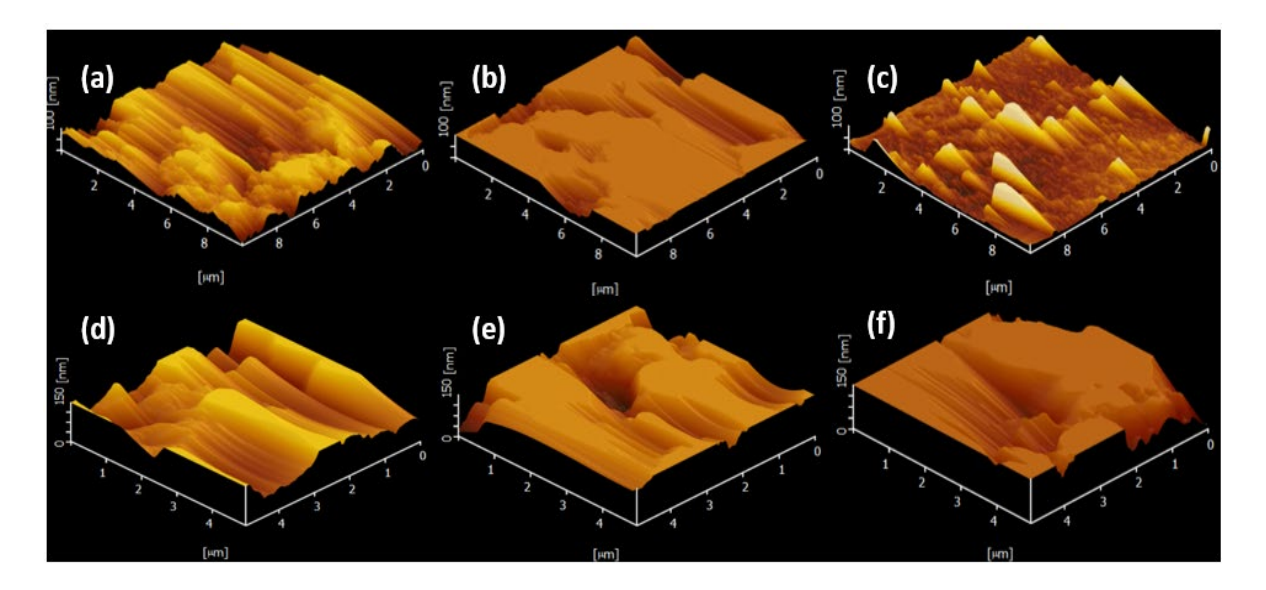


**Figure 3:** Surface topography (AFM) of samples using various molarity of stearic acid (a) 0.002 M, (b) 0.005 M, (c) 0.008 M, (d) 0.01 M, (e) 0.02 M and (f) 0.05 M

Table 2: Surface roughness	of samples	using various	molarity o	f stearic acid
----------------------------	------------	---------------	------------	----------------

Molarity (M)	Roughness Average, Ra (nm)	Root Mean Square, RMS (nm)	Roughness Factor (S-Ratio)
0.002	37.75	48.34	1.034
0.005	42.32	61.87	1.028
0.008	21.30	32.12	1.039
0.01	44.96	57.62	1.046
0.02	36.72	466.8	1.028
0.05	45.88	66.84	1.076

#### Corrosion Results

Figure 4 shows potentiodynamic polarization diagrams. All of the graphs show the same corrosion behavior. Lower corrosion potential ( $E_{corr}$ ) suggested a higher chance of corrosion [6]. Table 3 shows the corrosion rate calculated using Tafel extrapolation at various stearic acid concentrations. By comparing the different molarities of stearic acid, the corrosion rate reduces from 0.002 M to 0.008 M and begins to grow from 0.01 M to 0.05 M. This is due to the fact that 0.002 M and 0.005 M stearic acid are inadequate for the lamellar structure to completely cover the surface regions of the samples. Stearic acid at 0.008 M is adequate to cover the total surface area uniformly. As the stearic acid concentration increases, the excess stearate crystal and agglomeration with SiO<sub>2</sub> nanoparticles develop into uneven shapes, resulting in inconsistent corrosion resistance on the surface area. The chloride ion from the

electrolyte attacked the surface area with inadequate coverage of zinc stearate and agglomerated regions, resulting in a high corrosion rate.

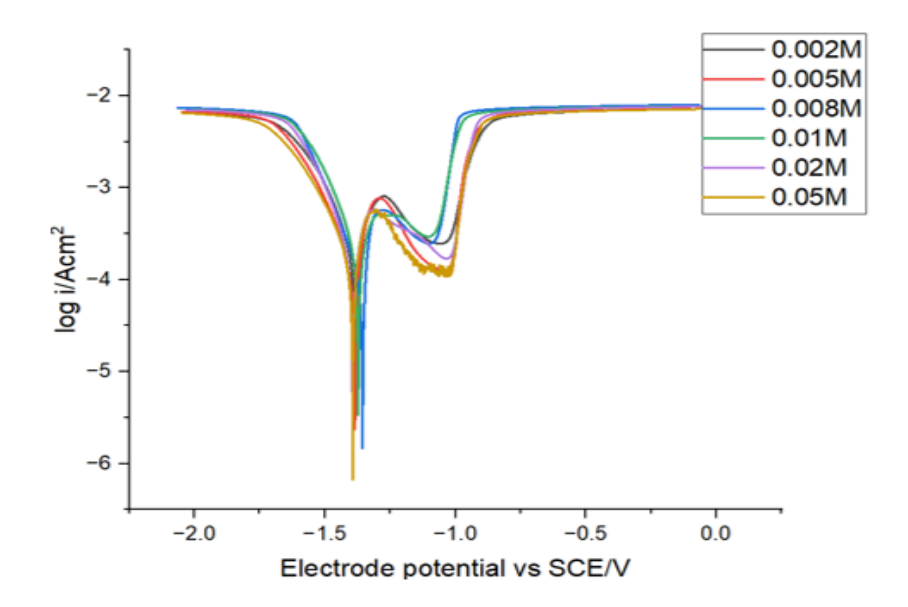


Figure 4: Tafel polarization graphs at different molarity of stearic acid

Table 3: Tafel corrosion results for different molarity of stearic acid

Molarity (M)	E <sub>corr</sub> (V)	<i>I<sub>corr</sub></i> (μ <b>A</b> )	Corrosion rate (mmyr <sup>-1</sup> )
0.002	-1.378	355.72	2.592
0.005	-1.387	151.96	1.771
0.008	-1.351	97.06	0.707
0.01	-1.371	89.47	1.043
0.02	-1.390	221.73	2.585
0.05	-1.392	266.37	4.532

## **Conclusions**

In this work, the effect of concentrations of stearic acid ranging from 0.002 to 0.05 M on surface modification of Zn-Al-WO<sub>3</sub> galvanised mild steel was examined. The 0.008 M stearic acid showed the most homogeneous zinc stearate distribution, with a maximum contact angle of 122.29° and the lowest surface energy of 10.42 mJ.m<sup>-2</sup>. Stearic acid concentration at this molarity also provided the lowest roughness surface and corrosion rate on galvanised Zn-Al-WO<sub>3</sub>, which were 21.30 nm and 0.707 mmyr<sup>-1</sup>, respectively. Modifying the surface of Zn-Al-WO<sub>3</sub> with 0.008 M stearic acid provides a greater proportion of air trap to lower the contact area between water and the Zn-Al-WO<sub>3</sub> galvanised coating. The modified surface of Zn-Al-WO<sub>3</sub> galvanised coating can provide hydrophobic and anti-corrosion for galvanised steel.

## Acknowledgements

The authors acknowledge and greatly appreciate for the administrative and infrastructural assistance provided by the School of Materials and Mineral Resources Engineering at Universiti Sains Malaysia and the financial support from University Grant 304/PBAHAN/6315676.

## **Author Contributions**

All authors contributed toward data analysis, drafting and critically revising the paper and agree to be accountable for all aspects of the work.

#### **Disclosure of Conflict of Interest**

The authors have no disclosures to declare.

# **Compliance with Ethical Standards**

The work is compliant with ethical standards.

## References

- [1] Shibli, S. M. A., Meena, B. N. & Remya, R. (2015). A Review on Recent Approaches in the Field of Hot Dip Zinc Galvanizing Process. *Surface and Coatings Technology*. 262, 210–215.
- [2] Polyakov, N. A., Botryakova, I. G., Glukhov, V. G., Red'kina, G. V. & Kuznetsov, Y. I. (2021). Formation and anticorrosion Properties of Superhydrophobic Zinc Coatings on Steel. *Chemical Engineering Journal*. 421, 127775.
- [3] Liu, Q., Zhang, X., Zhou, W., Ma, R., Du, A., Fan, Y., Zhao, X. & Cao, X. (2020). Improved Anti-corrosion Behaviour of an Inorganic Passive Film on Hot-dip Galvanised Steel by Modified Graphene Oxide Incorporation. *Corrosion Science*. 174, 108846.
- [4] Kania, H., Mendala, J., Kozuba, J. & Saternus, M. (2020). Development of Bath Chemical Composition for Batch Hot-dip Galvanizing-A Review. *Materials*. 13(18), 4168.
- [5] Arunima, S. R., Deepa, M. J., Elias, L., Sha, M. A., Sumi, V. S. & Riyas, A. H. (2022). Tuning of WO<sub>3</sub> Nanoparticles Integration into Fe–Zn Intermetallic Layers of Hot-dip Zinc Coating to Control Corrosion. *Materials Science and Engineering B: Solid-State Materials for Advanced Technology*. 276(January 2021), 115539.
- [6] Deepa, M. J., Arunima, S. R., Ramesh, H., Sumi, V. S., Sha, M. A. & Riyas, A. H. (2020). Tuning of Electrochemical and Topographical Characteristics for Enhancement of Anti-corrosion Performance of Hot-dip TiO<sub>2</sub>–Zn–(1%) Al Composite Coatings. *Corrosion Science*. 177(August 2020), 108944.

- [7] Arunima, S. R., Deepa, M. J., Geethanjali, C. V., Saji, V. S. & Shibli, S. M. A. (2020). Tuning of Hydrophobicity of WO<sub>3</sub>-based Hot-dip Zinc Coating with Improved Self-cleaning and Anti-corrosion Properties. *Applied Surface Science*. 527, 146762.
- [8] Arunima, S. R., Deepa, M. J., Nair, A. J. & Shibli, S. M. A. (2021). Exploration of WO<sub>3</sub>/BiVO<sub>4</sub> Composite Based Hot-dip Zinc Coating to Combat Biocorrosion. *Materials Science and Engineering B: Solid-State Materials for Advanced Technology*. 271(June 2021), 115302.
- [9] Zhou, W., Liu, S., DeFlorio, W., Song, S. H., Choi, H. & Cisneros-Zevallos, L. (2024). Nanostructured Antifouling Coatings for Galvanized Steel Food Storage and Container Surfaces to Enhance Hygiene and Corrosion Resistance Against Bacterial, Fungal, and Mud Contamination. *Journal of Food Engineering*. 363(October 2023), 111784.
- [10] Liang, T., Yuan, H., Li, C., Dong, S., Zhang, C. & Cao, G. (2021). Corrosion Inhibition Effect of Nano–SiO<sub>2</sub> for Galvanised Steel Superhydrophobic Surface. *Surface and Coatings Technology*. 406(November 2020), 108944.
- [11] Amanian, S., Naderi, R. & Mahdavian, M. (2023). Benzotriazole Modified Zn-Al Layered Double Hydroxide Conversion Coating on Galvanized Steel for Improved Corrosion. *Journal of the Taiwan Institute of Chemical Engineers*. 150(July 2023), 105072.
- [12] Naing, T. H., Janudom, S., Mahathaninwong, N., Limbut, W. & Karrila, S. (2023). Corrosion-resistant Superhydrophobic Films on Galvanised Steel by One-step Electrodeposition. *Materials Today Communications*. 35(May 2023), 106241.
- [13]Zhang, X. F., Chen, Y. Q. & Hu, J. M. (2020). Robust Superhydrophobic SiO<sub>2</sub>/Polydimethylsiloxane Films Coated on Mild Steel for Corrosion Protection. *Corrosion Science*. 166(July 2019), 108452.
- [14] Hu, C., Xie, X., Zheng, H., Qing, Y. & Ren, K. (2020). Facile Fabrication of Superhydrophobic Zinc Coatings with Corrosion Resistance by Electrodeposition Process. *New Journal of Chemistry*. 44(21), 8890–8901.
- [15] Hu, J., He, S., Wang, Z., Zhu, J., Wei, L. & Chen, Z. (2019). Stearic Acid-coated Superhydrophobic Fe<sub>2</sub>O<sub>3</sub>/Fe<sub>3</sub>O<sub>4</sub> Composite Film on N80 Steel for Corrosion Protection. *Surface and Coatings Technology*. 359(November 2018), 47–54.
- [16] Li, C., Ma, R., Du, A., Fan, Y., Zhao, X. & Cao, X. (2018). Superhydrophobic Film on Hot-dip Galvanised Steel with Corrosion Resistance and Self-cleaning Properties. *Metals*. 8(9), 687–703.
- [17] Gurav, A. B., Latthe, S. S., Vhatkar, R. S., Lee, J. G., Kim, D. Y. & Park, J. J. (2014). Superhydrophobic Surface Decorated with Vertical ZnO Nanorods Modified by Stearic Acid. *Ceramics International.* 40(5), 7151–7160.